J. Indian Inst. Sci., Mar.–Apr. 1996, **76**, 223–233.

Epitaxial nucleation and growth mechanism of III–V compound semiconductors

N. GOPALAKRISHNAN, R. S. QHALID FAREED AND R. DHANASEKARAN
Crystal Growth Centre, Anna University, Madras 600 025, India.

Received on August 9, 1994.

Abstract

An attempt has been made to investigate nucleation and growth mechanism of III–V compound semiconductors from vapour-phase epitaxy (VPE) and liquid-phase electroepitaxial (LPEE) growth techniques. Critical nucleation parameters have been derived using classical heterogeneous nucleation theory. The growth rate expressions have been developed in terms of input parameters for VPE and LPEE growth techniques. The model has been employed to understand the growth kinetics of quaternary $Ga_{1-x}In_xAs_{1-y}P_y$ in the In–Ga–HCl–PH_3–AsH_3–H_2 system during VPE growth and InAs during LPEE growth process. The effect of different experimental input parameters on the nucleation and growth behaviour have been studied in detail.

Keywords: Vapour-phase epitaxy, electroepitaxy, nucleation, gallium indium arsenide phosphide, compositions, concentration profiles, Peltier effect electromigration.

1. Introduction

In recent years, there has been tremendous development in the fabrication of electronic and optoelectronic device structures due to extensive work carried out for the growth of epilayers. Considering the recent trends from a technological point of view vapour-phase epitaxy (VPE) and liquid-phase electroepitaxy (LPEE) are found to be suitable methods to grow device-quality layers. In this communication, we report a model which has been developed to understand the nucleation and growth mechanism of VPE technique employed for the growth of $Ga_{1-y}In_yAs_{1-y}P_x$. A numerical model has been developed for InAs growth from liquid-phase electroepitaxy.

Though considerable work has been done on the deposition of $Ga_{1-y}In_yAs_{1-y}P_x$ layers[1, 2], vapour-phase epitaxial growth of this quaternary is still a challenging problem and its mechanism has not been investigated in detail[3]. Hence, fundamental investigations are necessary to understand the mechanism of deposition. Nucleation kinetics have been studied and critical nucleation parameters have been derived in terms of substrate supercooling and orientations. Vapour-phase epitaxial growth of quaternary $Ga_{1-y}In_yAs_{1-x}P_x$ is described by 19 equilibrium reactions. The expression for the compositions (x,y) of the alloy is derived as a function of input parameters.

Liquid-phase electroepitaxy is one of the novel techniques for the growth of compositionally uniform, controlled thickness and low dislocation ingots of III–V compound semiconductors. In this technique, under isothermal conditions, epilayers are grown by

passing an electric current through substrate–solution interface. The applied electric field is the main driving force for the growth of the epitaxial layers.

Due to several advantages of this technique over the conventional LPE, extensive experimental and theoretical work has been carried out by passing electric current in a modified LPE system[4–10]. A knowledge of concentration gradient of the solute atoms in front of the growing crystal–solution interface is very essential to understand the growth kinetics of the epilayers. In this communication, we present the theoretical model based on Peltier effect and electromigration to understand the growth kinetics of compound semiconductors by this novel technique.

2. Nucleation and growth kinetics

2.1. *Epitaxial nucleation of* $Ga_{1-y}In_yAs_{1-x}P_x$

Any quaternary alloy can be considered as the constituent of four binary compounds. The amount of free energy associated with the formation of $Ga_{1-y}In_yAs_{1-x}P_x$ nucleus containing a number of GaAs, b number of InAs, c number of GaP and d number InP molecules on the given substrate is[11],

$$\Delta G = -a\Delta\mu_{GaAs} - b\Delta\mu_{InAs} - c\Delta\mu_{GaP} - d\Delta\mu_{InP} + \pi r^2 \sin^2\theta(\sigma_{12} - \sigma_{23}) + 2\pi r^2(1-\cos\theta)\sigma_{13} \tag{1}$$

where $\Delta\mu_{GaAs}$, $\Delta\mu_{InAs}$, $\Delta\mu_{GaP}$ and $\Delta\mu_{InP}$ are the change in chemical potentials of GaAs, InAs, GaP and InP, respectively, σ_{23}, σ_{12} and σ_{13} are the surface-free energies per unit area between the substrate and gaseous mother phase, between the nucleus and substrate and between the nucleus and mother phase, respectively, and θ is the contact angle of the nucleus. The negative sign in eqn (1) indicates that the free energy change per unit volume of the nucleus is a negative quantity for the supersaturated system.

The critical radius

$$r^* = P\ \sigma_{13}/Q. \tag{2}$$

The number of $Ga_{1-y}In_yAs_{1-x}P_x$ molecules in the critical nucleus

$$a^* + b^* + c^* + d^* = \left(8\pi\ p^2\ \sigma_{13}^3/3Q^3\right)\left(2 - 3\cos\theta + \cos^3\theta\right). \tag{3}$$

The free energy formation of the critical nucleus is

$$\Delta G^* = \left(4\pi\ p^2\ \sigma_{13}^3/3Q^2\right)\left(2 - 3\cos\theta + \cos^3\theta\right), \tag{4}$$

where

$$P = (1-x)(1-y)\ V_{GaAs} + y(1-x)\ V_{InAs} + x(1-y)\ V_{GaP} + xy\ V_{InP}, \tag{5a}$$

$$Q = (1-x)(1-y)\ \Delta\mu_{GaAs} + y(1-x)\ \Delta\mu_{InAs} + x(1-y)\ \Delta\mu_{GaP} + xy\ \Delta\mu_{InP}, \tag{5b}$$

$$\theta = (1-x)(1-y)\ \theta_{GaAs} + y(1-x)\ \theta_{InAs} + x(1-y)\ \theta_{GaP} + xy\ \theta_{InP}, \tag{5c}$$

$$\sigma_{13}(111) = (1-x)(1-y)\ \sigma_{GaAs} + y(1-x)\ \sigma_{InAs} + x(1-y)\ \sigma_{GaP} + xy\ \sigma_{InP}, \tag{5d}$$

where V is the molar volume and x and y are the composition of phosphorus and indium in the quaternary alloy and these values are related to a, b, c and d through the relation

$$x = (c + d)/(a + b + c + d) \text{ and } y = (b + d)/(a + b + c + d).$$

In order to study the effect of orientation of the substrate on the nucleation parameters, the surface-free energy per unit area between substrate and gaseous mother phase, σ_{13}, should be evaluated as a function of orientation and it is given by[12],

$$\sigma_{13}(hkl) = [\Delta n(hkl)\, \rho(hkl)\, E_0/c], \tag{6a}$$

where $\Delta n(hkl)$ is the number of bonds broken, ρ, the density of face packing, E_0, the energy of the bond and c, the coordination number. The numerical values used for the zinc blend structure are

$$C = 4,\ \Delta n(100) = 2,\ \Delta n(110) = 1,\ \Delta n(100) = 1$$

$$\rho(100) = 2/a_c^2,\ \ \rho(110) = 4/a_c^2\ \sqrt{2},\ \ \rho(100) = 4/a_c^2\ \sqrt{3}$$

where a_c is the lattice constant. Assuming the coefficients of temperature dependence $d\sigma/dT$ to be equal, the surface free energy as a function of orientations[12] is given by

$$\sigma_{13}(111):\sigma_{13}(110):\sigma_{13}(100) = 1:1.2:1.7. \tag{6b}$$

The estimation of chemical potentials $\Delta\mu_{GaAs}$, $\Delta\mu_{InAs}$, $\Delta\mu_{GaP}$ and $\Delta\mu_{InP}$, are made as the product of the change in entropies Δs_{GaAs}, Δs_{InAs}, Δs_{GaP}, Δs_{InP} and substrate supercooling ΔT, respectively.

2.2. *Vapour-phase deposition of* $Ga_{1-y}In_yAs_{1-x}P_x$

The overall deposition of quaternary $Ga_{1-y}In_yAs_{1-x}P_x$ from the vapour phase can be written as

$$(1-y)GaCl(g) + yInCl(g) + (1-x)\ (1/4)\ As_4(g) + x(1/4)P_4(g)$$
$$+ (1/2)H_2(g) \overset{K}{\rightleftharpoons} Ga_{1-y}In_yAs_{1-x}P_x(s) + HCl(g). \tag{7}$$

It is considered that this reaction contains the following intermediate reactions during growth:

$$AsH_3(g) \overset{K_1}{\rightleftharpoons} (1/4)\ As_4(g) + (3/2)\ H_2(g) \tag{8}$$

$$PH_3(g) \overset{K_2}{\rightleftharpoons} (1/4)\ P_4(g) + (3/2)\ H_2(g) \tag{9}$$

$$(1/4)\ As_4(g) \overset{K_3}{\rightleftharpoons} (1/2)\ As_2(g) \tag{10}$$

$$(1/4)\ P_4(g) \overset{K_4}{\rightleftharpoons} (1/2)\ P_2(g) \tag{11}$$

$$(1/2)\ As_2(g) + * \overset{K_5}{\rightleftharpoons} As* \tag{12}$$

$$(1/2)\ P_2(g) + * \overset{K_6}{\rightleftharpoons} P* \tag{13}$$

$$GaCl\ (g) + * \overset{K_7}{\rightleftharpoons} Gacl* \tag{14}$$

$$InCl(g) + {}^{K_8}\rightleftharpoons InCl^* \tag{15}$$

$$As^* + GaCl(g) \overset{K_9}{\rightleftharpoons} AsGaCl^* \tag{16}$$

$$As^* + InCl(g) \overset{K_{10}}{\rightleftharpoons} AsInCl^* \tag{17}$$

$$P^* + GaCl(g) \overset{K_{11}}{\rightleftharpoons} PGaCl^* \tag{18}$$

$$P^* + InCl(g) \overset{K_{12}}{\rightleftharpoons} PInCl^* \tag{19}$$

$$AsGaCl^* + (1/2)\, H_2(g) \overset{K_{13}}{\rightleftharpoons} GaAs^* + HCl(g) \tag{20}$$

$$AsInCl^* + (1/2)\, H_2(g) \overset{K_{14}}{\rightleftharpoons} InAs^* + HCl(g) \tag{21}$$

$$PGaCl^* + (1/2)\, H_2(g) \overset{K_{15}}{\rightleftharpoons} GaP^* + HCl(g) \tag{22}$$

$$PInCl^* + (1/2)\, H_2(g) \overset{K_{16}}{\rightleftharpoons} InP^* + HCl(g) \tag{23}$$

$$xy\, InP^* + x(1-y)\, GaP^* + y(1-x)\, InAs^* + (1-x)(1-y)\, GaAs^* \overset{K_{17}}{\rightleftharpoons} Ga_{1-y}In_yAs_{1-x}P_x^* \tag{24}$$

$$Ga_{1-y}In_yAs_{1-x}P_x^* \overset{K_{18}}{\rightleftharpoons} Ga_{1-y}In_yAs_{1-x}P_x^*(s) + * \tag{25}$$

where * denotes the vacant site for adsorption and the subscript g is used for gaseous state and s for solid state. The equilibrium constants for these reactions are taken from literature[12–16]

Assuming the formation of the complex molecules AsGaCl, AsInCl, PGaCl, PInCl as the rate-determining steps, the growth of respective binary which are constituents of quaternary can be written in terms of partial pressure as

$$R_{GaAs} = \frac{K_1K_3K_5K_9\, p_{AsH_3}p_{GaCl}}{p_{H_2}^{3/2}\left(1 + K_1K_3K_5\, p_{AsH_3}/p_{H_2}^{3/2} + K_7\, p_{GaCl} + K_1K_3K_5K_9\, p_{AsH_3}\cdot p_{GaCl}/p_{H_2}^{3/2} + K_1K_3K_5K_9K_{13}\cdot p_{GaCl}\, p_{AsH_3}/p_{HCl}\, p_{H_2}\right)} \tag{26}$$

Similarly, the growth rate of other binaries (InAs, GaP, InP) are also derived. The growth rate R of the quaternary GaInAsP can be expressed as the sum of the deposition rates of four binaries as

$$R_{GaInAsP} = R_{GaAs} + R_{InAs} + R_{GaP} + R_{InP}. \tag{27}$$

Hence the phosphorus (x) composition in the $Ga_{1-y}In_yAs_{1-x}P_x$ alloy is

$$x = \frac{\left(R_{GaP} + R_{InP}\right)}{R_{GaInAsP}}; \tag{28}$$

and the composition of indium is

$$y = \frac{\left(R_{InAs} + R_{InP}\right)}{R_{GaInAsP}} \tag{29}$$

2.3. *Liquid-phase electroepitaxial growth model for InAs*

In the present work, the diffusion treatment equation in the conventional LPE process has been modified to incorporate the electromigration effect. The mobility μ and the applied electric field E in the melt have significant contributions in the electromigration of the solute species. The direction of the applied electric field induces either Peltier cooling or Peltier heating at the solution–substrate interface. The one-dimensional equation for the electroepitaxial system can be written as[10]

$$D\frac{\partial^2 C}{\partial z^2} - v\frac{\partial C}{\partial z} \pm \mu E\frac{\partial C}{\partial z} = \frac{\partial C}{\partial t}, \tag{30}$$

where D and μ are the diffusion coefficient and mobility of As in molten In; v, the growth velocity of the interface and C, the As concentration. (The sign $\pm$ of the electromigration term is determined by the direction of the current flow)

Assuming, for the case of LPEE growth,

$$v\frac{\partial C}{\partial z} \ll D\frac{\partial^2 C}{\partial z^2}, \tag{31}$$

(30) can be written as

$$D\frac{\partial^2 C}{\partial z^2} \pm \mu E\frac{\partial C}{\partial z} = \frac{\partial C}{\partial t}. \tag{32}$$

In the present calculations, we have followed the methods of Crossley and Small[17] to calculate the concentration of the solute atoms in front of the growing crystal. The solution in front of the InAs crystal interface in the LPEE system has been segmented into 30 segments of width ϵ and each segment has the concentration C_1, C_2, ..C_j,..C_{30} at any given time (where $j = 1$ to 30 is the segment number). The following boundary conditions are applied to simulate the concentration profiles,

At $t = 0$,	$C = C_0$	for all z		(33a)
At $t > 0$	$C = C_0$	for $z = 30\epsilon$	(in the absence of convection)	(33b)
or				
At $t > 0$	$C = C_0$	for $z = \delta$	(in the presence of convection)	(33c)
At $t > 0$ and $z = 0$,	$C = C_1$		(growth follows the liquidus line)	(33d)

where C_0 is the equilibrium concentration at 620°C, C_1, the concentration of the solute species near the interface and z, the distance from the advancing growth interface. The concentration of the As atoms at the equilibrium conditions can be determined at a temperature of 620°C from the equation

$$C_0 = 5.11 \times 10^{22} \exp[8.429 - (1.0602 \times 10^4)/T]. \tag{34}$$

The change in the concentration in the jth segment due to the Peltier effect and electromigration at the next step is obtained by solving eqn (32) and can be given as[18, 19]

$$C_{j,n+1} = C_{j,n} + \frac{D\tau}{\epsilon^2}\left(C_{j-1,n} - 2C_{j,n} + C_{j+1,n}\right) \pm \frac{\mu E \tau}{2\epsilon}\left(C_{j+1,n} - C_{j-1,n}\right), \tag{35}$$

where τ is a small time step taken for the growth of epitaxial layers. Simulations of the concentration of the solute atoms for successive intervals of time at constant temperature and electric field have been carried out to understand the growth mechanism in In–As system.

Growth/dissolution rates of the epilayers have been calculated during the electroepitaxial growth of semiconductors. In the absence of convection, growth/dissolution rates can be given as

$$v = \frac{\Delta T_p m (D/\pi t)^{1/2} - \mu E\, C_L(t)}{C_s - C_1}. \tag{36}$$

In the presence of convection

$$v = \frac{\Delta T_p m (D/\delta)^{1/2} - \mu E\, C_L(t)}{C_s - C_1}, \tag{37}$$

where $m = dC/dT$, ΔT_p is the change in interface temperature, δ, the thickness of solute boundary layer, C_s, the concentration in the solid and $C_L(t)$, the concentration at liquid.

3. Results and discussion

Let p_{HCl} (1) and p_{HCl} (2) be the partial pressures of HCl introduced into the molten Ga and In, respectively, to produce III group monochlorides (GaCl, InCl).

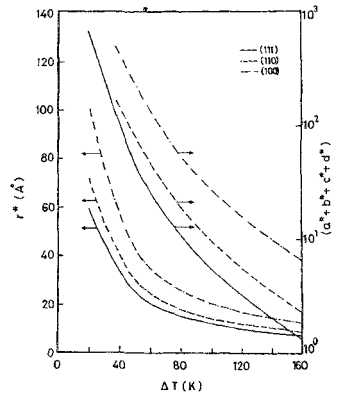

FIG. 1. Critical size and number of GaInAsP molecules in the critical nucleus as a function of supercooling for different orientations of the substrate surface.

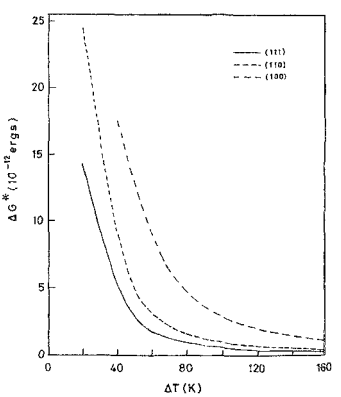

FIG. 2. Critical free energy barrier of GaInAsP nucleus *vs* supercooling for different orientations of the substrate surface.

Figure 1 shows the critical radius and the number of GaInAsP molecules in the critical nucleus in $Ga_{.65}In_{.35}As_{.21}P_{.79}$ alloy as a function of supercooling. The (111) orientation has the lowest values of the nucleation parameters.

Figure 2 shows the critical free energy barrier for the formation of $Ga_{.65}In_{.35}As_{.21}P_{.79}$ nucleus as a function of supercooling. For a particular supercooling, the (100) orientation gives the highest free energy barrier for the formation of $Ga_{.65}In_{.35}As_{.21}P_{.79}$ nucleus.

Figure 3 shows the calculated crystal composition x as a function of partial pressure ratio $p_{PH_3}/(p_{PH_3}+p_{AsH_3})$ for various deposition temperatures. The phosphorus composition in the alloy increases with increase in the deposition temperature. The dependence of the indium composition in the quaternary alloy grown on the mole ratio $p_{HCl}(1)/(p_{HCl}(1)+p_{HCl}(2))$ for various values of phosphorus mole ratio is shown in Fig. 4. The calculated input partial pressures of the constituent species for various solid compositions x of $Ga_{1-y}In_yAs_{1-x}P_x$ alloy are shown in Fig. 5. From this numerical chart it is possible to determine the exact experimental conditions for the growth of alloy of desired compositions.

Computer simulation technique has been employed to construct the concentration profiles of As in the In-rich melt during InAs growth. The effect of Peltier cooling and Peltier heating caused due to the application of electric field between the substrate–solution interface has been incorporated in constructing the concentration profiles of As

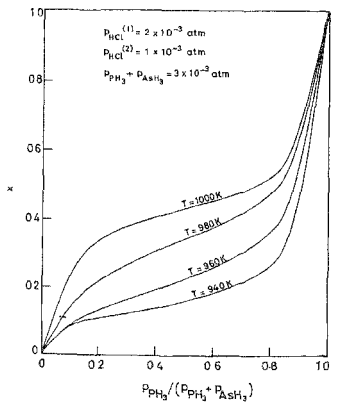

FIG. 3. Effect of mole ratio $p_{PH_3}/(p_{PH_3}+p_{AsH_3})$ on the composition x and y of $Ga_{1-y}In_yAs_{1-x}P_x$ alloy.

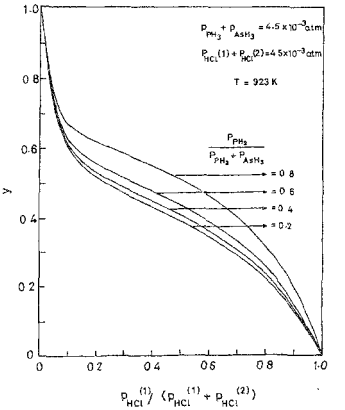

FIG. 4. Indium composition *vs* $P_{HCl}(1)/[p_{HCl}(1)+p_{HCl}(2)]$ *mole ratio* for different experimental conditions.

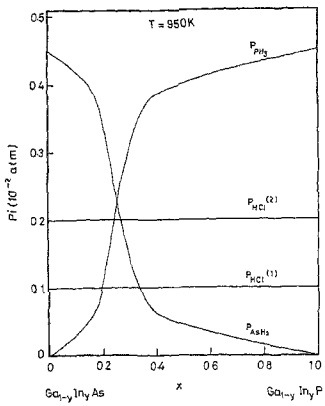

FIG. 5 Calculated partial pressures of different species inside the reactor for the growth of quaternary $Ga_{1-y}In_yAs_{1-x}P_x$ alloy as a function of phosphorus composition x.

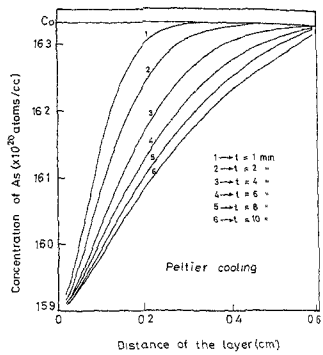

FIG. 6. Concentration profiles of As during electroepitaxial growth of InAs during Peltier cooling for different intervals of time.

species. Figures 6 and 7 show the concentration profiles of As in In-rich melt for different intervals of time during Peltier cooling and Peltier heating at the interface assuming $\Delta T_p = \pm 2°C$, solution height of 0.6 cm, diffusion coefficient of As species as 8.241×10^{-5} cm^2/s and an applied current density of 10 A/cm^2. Due to Peltier cooling, there is a supersaturation which leads to the growth of epilayers over the substrate. Hence, there is a decrease in the concentration of p near the interface as shown in Fig. 6. During Peltier heating, the concentration of the solute atoms increases near the interface due to dissolution of the substrate and grown epilayers with time as shown in Fig. 7.

Concentration profiles have been constructed in the solution for different values of applied electric field μE when time $t = 5$ min (Fig. 8). It is observed that there is a decrease in the concentration of As atoms as the applied electric field is increased due to growth caused by Peltier cooling. Also there is dissolution at the interface due to Peltier heating when the direction of the applied electric field is reversed which increases the concentration of As atoms near the interface as the electric field is increased.

In Fig. 9, concentration profiles for different values of change in interface temperature ΔT_p have been shown when $t = 5$ min. The concentration of As atoms decreases due to Peltier cooling as the change in interface temperature increases. Also there is an increase in the concentration of As atoms due to dissolution as the interface temperature increases due to Peltier heating.

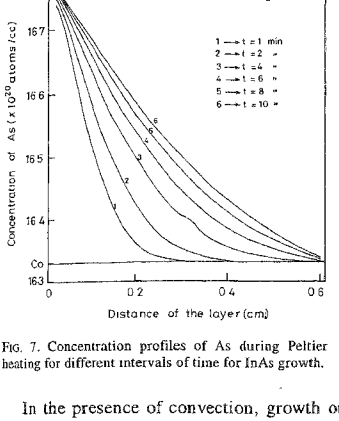

FIG. 7. Concentration profiles of As during Peltier heating for different intervals of time for InAs growth.

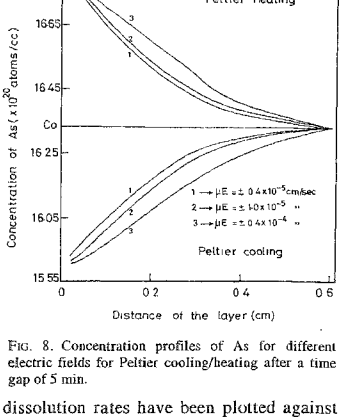

FIG. 8. Concentration profiles of As for different electric fields for Peltier cooling/heating after a time gap of 5 min.

In the presence of convection, growth or dissolution rates have been plotted against change in the interface temperature ΔT_p for different values of solute boundary layer thickness δ formed due to the presence of convection (Fig. 10). As the thickness of the boundary layer decreases, there is an increase in the deposition or dissolution rate of the epitaxial layers. At larger thickness of solute boundary layers at the solution–substrate interface, the growth/dissolution rates decrease with change in interface temperature.

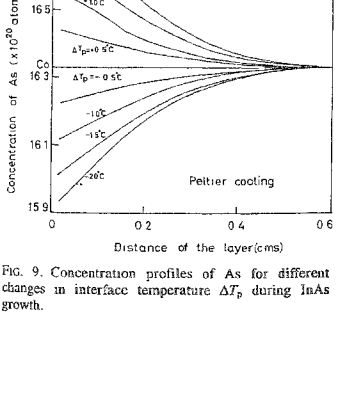

FIG. 9. Concentration profiles of As for different changes in interface temperature ΔT_p during InAs growth.

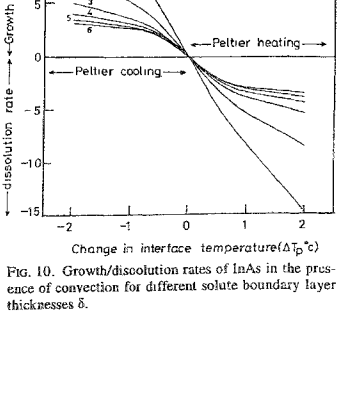

FIG. 10. Growth/dissolution rates of InAs in the presence of convection for different solute boundary layer thicknesses δ.

Typical values used for the growth of quaternary alloy are:

$\sigma_{GaAs} = 250$ erg cm^{-2} $\sigma_{InAs} = 350$ erg cm^{-2}
$\sigma_{GaP} = 300$ erg cm^{-2} $\sigma_{InP} = 200$ erg cm^{-2}
for (111) orientations
$\Delta S_{GaAs} = 32.17$ cal mol^{-1} K^{-1} $\Delta S_{InAs} = 28.23$ cal mol^{-1} K^{-1}
$\Delta S_{GaP} = 27.27$ cal mol^{-1} K^{-1} $\Delta S_{InP} = 33.40$ cal mol^{-1} K^{-1}
$\theta_{GaAs}\theta = 40.54°$ $\theta_{GaP} = 36.87°$, $\theta_{InP} = 45.57°$
$\theta_{InAs} = 34.05°$

4. Conclusion

A kinetic model has been developed to understand the nucleation and growth mechanism of vapour-phase epitaxial growth of quaternary $Ga_{1-y}In_yAs_{1-x}P_x$ alloy and electroepitaxial growth of InAs. The orientation effects on the critical nucleation parameters are studied. The expressions for the solid compositions are deduced from the growth rate expressions. The effect of different experimental input parameters on the composition is studied. Concentration profiles of the solute atoms during InAs electroepitaxial growth have been constructed using computer simulation technique for different experimental conditions. Growth/dissolution rates have been calculated in the presence of convection. Thus, the developed model accounts for different experimental conditions for the suitability of epitaxial layers for device applications.

Acknowledgement

RD is grateful to Dr S. Lourdudoss, Royal Institute of Technology, Kista, Sweden, for the useful discussion on the VPE of quaternary system.

References:

1. Sugiyama, K., Kojima, H., Enda, H and Shibata, M. *Jap. J. Appl Phys.*, 1977, **16**, 2197–2203.
2. Hyder, S. B., Saxena, R.R. and Hooper, C.C. *Appl. Phys. Lett.*, 1979, **34**. 584–586.
3. Ikeda, H., Nishiyama, Y., Kouketu, A. and Seki, H. *J. Cryst. Growth*, 1992, **123**, 213–220.
4. Kumagawa, M., Witt, A. F., Lichtensteiger, M. and Gatos, H. C. *J. Electrochem Soc* . 1973, **120**, 583–584.
5. Jastrzebski, L., Imamura, Y. and Gatos, H. C. *J. Electrochem. Soc.*, 1978, **125**. 1140–1146.
6. Bryskiewicz, T. *Prog. Cryst. Growth Characterisation*, 1986, **12**, 29–43
7. Yanagase, M., Tanaka, S., Hiramatsu, K. and Akasaki, I. *J. Cryst. Growth*, 1991, **115**, 304–308.
8. Bryskiewicz, T. *et al.* *J. Appl Phys.*, 1990, **68**, 3018–3020

9. BRYSKIEWICZ, T. AND LAFERRIERE, A. — *J. Cryst Growth*, 1993, **129**, 429–442.

10. JASTRZEBSKI, L., LAGOWSKI, J., GATOS, H.C. AND WITT, A.F. — *J Appl. Phys*, 1978, **49**, 5909–5919.

11. DHANASEKARAN, R. — Ph. D. thesis, Anna University, Madras, India, 1984.

12. MANI, V.N., DHANASEKARAN, R. AND RAMASAMY, P — *Semicond. Sci. Technol.*, 1987, **12**, 73–77.

13. KOREC, J, AND HEYAN, H. — *J. Cryst Growth*, 1982, **60**, 297–306.

14 MANI, V. N., DHANASEKARAN, R. AND RAMASAMY, P — *Thin Solid Films*, 1988, **163**,437–441.

15. GOPALAKRISHNAN, N. AND DHANASEKARAN, R. — *J. Cryst. Growth* (communicated).

16. MANI, V N., DHANASEKARAN, R AND RAMASAMY, P. — *J Appl. Phys.*, 1990, **69**, 1399–1406.

17. CROSSLEY, I. AND SMALL, M.B — *J Cryst. Growth*, 1991, **11**, 157–165.

18. QHALID FAREED, R. S., DHANASEKARAN, R. AND RAMASAMY, P. — *J. Appl. Phys*, 1994, **75**, 3953–3958.

19. QHALID FAREED, R. S., DHANASEKARAN, R. AND RAMASAMY, P. — *J Cryst. Growth*, 1994, **140**, 28–32.